Numerical cubature on scattered data by radial basis functions

A. Sommariva, Sydney, and **M. Vianello**, Padua

September 5, 2005

Abstract

We study cubature formulas on relatively small scattered samples in the unit square, obtained by integrating radial basis function (RBF) interpolants. Numerical tests show that, due to the small size of the corresponding weights (which are not all positive in general), thin-plate splines and Wendland's compactly supported radial functions give the most reliable RBF cubature methods.

AMS Subject Classification: 65D05, 65D32.
Key words: numerical integration, scattered data, radial basis functions.

1 Introduction.

In this paper we explore the use of the potentialities and the drawbacks of numerical cubature by radial basis functions (RBF). The idea of using RBF to construct cubature formulas on scattered samples is certainly not new (see, e.g., [6]), but to our knowledge does not seem to have received a systematic treatment in the numerical literature.

The problem itself of cubature on scattered points has received very limited attention with respect to the construction of cubature formulas on nodes with a predefined distribution [10].

On the other hand, integration of radial kernels in presence of boundaries is an important issue for the solution of PDE by *meshless methods* [11]. We mention in particular the works by Atluri and collaborators on the "meshless local Petrov Galerkin" (cf., e.g. [2]) and the "volume integral formulation" of the time dependent conservation equations proposed in [19].

Indeed, during the last two decades radial basis function interpolation has been developed as a powerful and popular tool for the recovery of multivariate functions from *scattered* data, with a vast body of literature on both the theoretical and the computational features; see, e.g., the survey papers [7, 26], and the recent monographs [8, 18, 29]. We will now briefly sketch the cubature method which can be generated by RBF interpolation, which

of course strictly follows the well-known approach for deriving quadrature formulas from polynomial interpolation.

Suppose that we are given a scattered sample of size n

$$\mathbf{f} = \{f(P_i)\} \text{ at } X = \{P_i\} = \{(x_i, y_i)\} \subset \Omega \,, \quad i = 1, \ldots, n \,, \tag{1}$$

of a given continuous function f on a multivariate compact set $\Omega \subset \mathbf{R}^N$ (the closure of an open and bounded set), and that we need to compute an approximate value of the integral

$$I(f) = \int_\Omega f(P)\, dP \,. \tag{2}$$

Once we have fixed a suitable radial function $\phi : [0, +\infty) \to \mathbf{R}$, we can construct the RBF interpolant at the points $\{P_i\}$

$$\sum_{j=1}^{n} c_j\, \phi_j(P) = s(P) \approx f(P) \,, \quad P = (x, y) \in \Omega \,, \tag{3}$$

where $s(P_i) = f(P_i)$, $i = 1, \ldots, n$, as a linear combination of (scaled) translates of ϕ

$$\phi_j(P) = \phi_j(P; \delta) := \phi(|P - P_j|/\delta) \,, \tag{4}$$

$|P - P_j|$ denoting the euclidean distance, and δ a scaling parameter, which can be related to the data density. The coefficients $\mathbf{c} = \{c_j\}$ are computed by solving the linear system

$$A\mathbf{c} = \mathbf{f} \qquad \text{(interpolation equations)} \,, \tag{5}$$

where

$$A = A_{X,\phi} = \{\phi_j(P_i)\}_{1 \le i,j \le n} \tag{6}$$

is a symmetric matrix, usually termed collocation matrix of the RBF. Clearly, a key point is the non-singularity of A, which depends on the choice of ϕ. In this paper, we consider some of the most popular choices, like

- Gaussians (G): $\phi(r) = \exp(-r^2)$
- Duchon's Thin-Plate Splines (TPS): $\phi(r) = r^2 \log(r)$
- Hardy's MultiQuadrics (MQ): $\phi(r) = (1 + r^2)^{1/2}$
- Inverse MultiQuadrics (IMQ): $\phi(r) = (1 + r^2)^{-1/2}$
- Wendland's compactly supported (W2): $\phi(r) = (1 - r)_+^4 (4r + 1)$

We recall that G, IMQ and W2 are *positive definite* (PD), i.e. the corresponding collocation matrix A is positive definite for every choice of the (distinct) interpolation nodes, while TPS and MQ are *conditionally* positive definite (CPD). In the latter cases, as is well-known [8], the RBF interpolant is sought in the form

$$s(P) = \sum_{j=1}^{n} c_j \, \phi_j(P) + p_m(P) \; , \tag{7}$$

where $p_m(P) = \sum_{k=1}^{M} b_k \pi_k(P)$ is a suitable polynomial of degree $\leq m$, M being the dimension and $\{\pi_k\}$ a basis of the corresponding bivariate polynomial space ($m = 1$, $M = 3$ for TPS and $m = 0$, $M = 1$ for MQ). The system (5) is then substituted by the augmented system of dimension $n + M$, $A\mathbf{c} + P\mathbf{b} = \mathbf{f}$, $P^T\mathbf{b} = \mathbf{0}$, where $P_{kj} = \pi_k(P_j)$.

Now, it is natural to approximate the integral $I(f)$ in (2) as

$$I(f) \approx I(s) = \sum_{j=1}^{n} c_j \, I(\phi_j) + I(p_m) \; ,$$

$$I(p_m) = \int_\Omega p_m(P) \, dP \; , \quad I(\phi_j) = \int_\Omega \phi_j(P) \, dP \; , \quad j = 1, \ldots, n \; , \tag{8}$$

where $p_m \equiv 0$ in positive definite instances. It is immediately seen that the cubature formula (8) can be rewritten in the usual form of a weighted sum of the sample values. In fact, confining for simplicity to the positive definite case, we have by symmetry of A

$$I(f) \approx I(s) = \langle \mathbf{c}, \mathbf{I} \rangle = \langle A^{-1}\mathbf{f}, \mathbf{I} \rangle = \langle \mathbf{f}, \mathbf{w} \rangle = \sum_{j=1}^{n} w_j \, f_j \; , \tag{9}$$

$$A\mathbf{w} = \mathbf{I} \; , \quad \text{with} \;\; \mathbf{I} = \{I(\phi_j)\}_{1 \leq j \leq n} \qquad \text{(cubature equations)} \tag{10}$$

where $\langle \cdot, \cdot \rangle$ denotes the scalar product in $\mathbf{R}^N$, and $\mathbf{I}$ the vector of integrals on Ω of the radial basis functions.

As for the convergence of the method, using the Hölder inequality we can write

$$\begin{aligned} |I(f) - I(s)| &\leq \|f - s\|_{L^1(\Omega)} \leq \sqrt{\mathrm{meas}(\Omega)} \, \|f - s\|_{L^2(\Omega)} \\ &\leq \mathrm{meas}(\Omega) \, \|f - s\|_\infty \; , \end{aligned} \tag{11}$$

and thus using known estimates for L^2 or for uniform convergence of RBF interpolation [8, 29, 30], we get

$$I(f) = I(s) + \mathcal{O}(\alpha(h)) \; , \quad \alpha(h) \to 0 \;\; \text{as} \;\; h \to 0 \; ,$$

$$h = \max_{P \in \Omega} \min_{1 \leq j \leq n} |P - P_j| \; , \tag{12}$$

where h is the so-called *fill distance* of the interpolation points, that is the radius of the largest inner empty disk. The convergence rate depends on the regularity degree of both the chosen radial basis function and the sampled function f: for f sufficiently regular (technically, belonging to the "native space" of the given RBF) the bound $\alpha(h)$ may *decrease exponentially* (C^∞ RBF like G, MQ, IMQ), or *algebraically* (less smooth RBF like TPS, W2), as $h \to 0$. We recall that another technical assumption is used in the literature to get the quoted convergence result, i.e. the requirement that the set Ω satisfies an *interior cone condition*, cf., e.g., [8, 18, 25].

The convergence analysis above seems promising, but is too rough to give useful information for the implementation. First, any serious analysis of a cubature formula has to do with the quantity $\sum |w_j|$, which plays a central role both in the study of the cubature error, and in the effect of perturbations (e.g. noise) in the sample values. Moreover, as is usual in the RBF framework, big trouble can arise from the computational point of view in evaluating the relevant coefficients. In fact, in any implementation the integrals $\mathbf{I} = \{I(\phi_j)\}_{1 \le j \le n}$ have to be approximated, and such errors are transmitted to the computed weights via the numerical solution of the linear system (5). Unfortunately, such a system can be (even extremely) ill-conditioned (depending on the data density and the chosen RBF), and a sort of dichotomy appears, termed "*uncertainty principle*" in Schaback's basic papers on RBF interpolation, which can be briefly summarized using directly Schaback's words [25]: "*There is no case known where the errors and the sensitivity are both reasonably small*".

In the next Section, we try to give a more refined error analysis of RBF cubature, which tries to take into account the role of important parameters, like $\sum |w_j|$ and $\|A^{-1}\|_2$. Such parameters will be estimated a posteriori during the computation, and will appear in the tables of the numerical results (Section 4). In Section 3, we give details on the implementation of RBF cubature, in particular concerning the evaluation of the integrals $\mathbf{I} = \{I(\phi_j)\}_{1 \le j \le n}$ via polar coordinates on the unit square, by exploiting the radial symmetry.

2 Error analysis.

In this Section we deepen the error analysis in RBF cubature formulas like (9)-(10); for simplicity, we restrict again the analysis to the *positive definite* case. In particular, we take into account the unavoidable errors in the evaluation of the integrals of the radial basis functions, i.e. the fact that we have at hand in practice a vector of *approximate integrals*

$$\{\tilde{I}(\phi_j)\} = \tilde{\mathbf{I}} \approx \mathbf{I}\,, \tag{13}$$

which generates a vector of *approximate weights* and a perturbed cubature formula (cf. (10))

$$\langle \mathbf{c}, \tilde{\mathbf{I}} \rangle = \langle \tilde{\mathbf{w}}, \mathbf{f} \rangle = \sum_{j=1}^{n} \tilde{w}_j \, f_j \approx \langle \mathbf{w}, \mathbf{f} \rangle = I(s) \approx I(f) \ , \quad \text{where } \ \tilde{\mathbf{w}} = A^{-1} \tilde{\mathbf{I}} \ . \tag{14}$$

A first error estimate is given in the following

Proposition 1 *The error of the RBF cubature formula* (9)-(10)*, in the presence of approximate values of the basis functions integrals* (*see* (13)-(14))*, can be estimated as*

$$\begin{aligned} |I(f) - \langle \tilde{\mathbf{w}}, \mathbf{f} \rangle| &\leq \text{meas}(\Omega) \, \|f - s\|_\infty + \|A^{-1}\|_2 \, \|\mathbf{f}\|_2 \, \|\mathbf{I} - \tilde{\mathbf{I}}\|_2 \\ &= \mathcal{O}(\alpha(h)) + \mathcal{O}(\beta(q)) \, \|\mathbf{I} - \tilde{\mathbf{I}}\|_2 \ , \end{aligned} \tag{15}$$

where $\alpha(h) \to 0$ *as* $h \to 0$*, and* $\beta(q) \to +\infty$ *as* $q \to 0$*,* h *denoting the fill distance in (12) and* q *the separation distance*

$$q = \min_{i \neq j} \{|P_i - P_j|\} \leq 2h \ . \tag{16}$$

Before proving Proposition 1, it is worth making a remark on the role of $\|A^{-1}\|_2$ and the meaning of (15).

Remark 2.1 The parameter $\|A^{-1}\|_2$ is a measure of the sensitivity to perturbations of the RBF approximation process. Starting from some basic papers at the beginning of the '90s (see, e.g., [22, 3, 4]), lower bounds for the smallest eigenvalue of the collocation matrix A (augmented in CPD instances) have been extensively studied in the RBF literature (see, e.g., [8, 18, 25, 28, 29] and references therein), providing upper bounds for $\|A^{-1}\|_2$ like

$$\|A^{-1}\|_2 = \mathcal{O}(\beta(q)) \ , \quad \beta(q) \to +\infty \ \text{ as } \ q \to 0 \ . \tag{17}$$

The fact that $\|A^{-1}\|_2$ diverges as $q \to 0$ is natural, since A tends to become singular when two rows collapse. We recall that the growing rate of β depends, as the convergence rate α in (11), on the smoothness degree of the chosen RBF: the bound $\beta(q)$ may *increase algebraically* (TPS, W2), or *exponentially* (G, MQ, IMQ), as $q \to 0$. Estimate (15) expresses, in the cubature context, just the *uncertainty principle* of RBF approximation quoted above. Observe that the rates of α and β are both algebraic, or both exponential. The situation seems hopeless concerning the use of smooth RBF like Gaussians for numerical cubature, in view of the expected exponential magnification of the integration errors, but the numerical results show that (15) is a quite pessimistic bound.

Proof of Proposition 1. Starting from (9)-(11), we obtain a first estimate

$$\begin{aligned} |I(f) - \langle \tilde{\mathbf{w}}, \mathbf{f} \rangle| &\leq |I(f) - \langle \mathbf{w}, \mathbf{f} \rangle| + |\langle \mathbf{w} - \tilde{\mathbf{w}}, \mathbf{f} \rangle| \\ &= |I(f) - I(s)| + |\langle A^{-1}(\mathbf{I} - \tilde{\mathbf{I}}, \mathbf{f}) \rangle| \\ &\leq \|f - s\|_{L^1(\Omega)} + \|A^{-1}(\mathbf{I} - \tilde{\mathbf{I}})\|_2 \, \|\mathbf{f}\|_2 \leq E_1 + E_2 \, , \end{aligned} \tag{18}$$

where we have set

$$E_1 = \mathrm{meas}(\Omega) \, \|f - s\|_\infty \, , \;\; E_2 = \|A^{-1}\|_2 \, \|\mathbf{f}\|_2 \, \|\mathbf{I} - \tilde{\mathbf{I}}\|_2 \, . \tag{19}$$

From (17) and the convergence results recalled in writing (12), we get (15). □

We derive now a second error estimate, where is clarified the role of the crucial parameter $\|\mathbf{w}\|_1 = \sum_{j=1}^n |w_j|$, that is the norm of the RBF cubature *functional* $C(\Omega) \to \mathbf{R}$, $f \mapsto \langle \mathbf{w}, \mathbf{f} \rangle$. Here, we take also into account the effect of perturbations (e.g. *noise*) on the sample values, i.e. the fact that we work in practice with a *perturbed sample*

$$\{\tilde{f}(x_j)\} = \tilde{\mathbf{f}} \approx \mathbf{f} \, . \tag{20}$$

Proposition 2 *The error of the perturbed RBF cubature formula* $\langle \tilde{\mathbf{w}}, \tilde{\mathbf{f}} \rangle$ (*cf.* (14), (20)) *can be estimated as*

$$\begin{aligned} |I(f) - \langle \tilde{\mathbf{w}}, \tilde{\mathbf{f}} \rangle| &\leq (\mathrm{meas}(\Omega) + \|\mathbf{w}\|_1) \; E_{X,\phi}(f) + \|\mathbf{w}\|_1 \, \|\mathbf{f} - \tilde{\mathbf{f}}\|_\infty \\ + \|A^{-1}\|_2 \, \|\mathbf{f}\|_2 \, \|\mathbf{I} - \tilde{\mathbf{I}}\|_2 \, , \;\; &\text{where} \;\; E_{X,\phi}(f) = \inf_{z \in span\{\phi_j\}} \{\|f - z\|_\infty\} \, . \end{aligned} \tag{21}$$

Proof. Starting from

$$\begin{aligned} |I(f) - \langle \tilde{\mathbf{w}}, \tilde{\mathbf{f}} \rangle| &\leq |I(f) - \langle \mathbf{w}, \mathbf{f} \rangle| + |\langle \mathbf{w}, \mathbf{f} \rangle - \langle \tilde{\mathbf{w}}, \tilde{\mathbf{f}} \rangle| \\ &\leq |I(f) - \langle \mathbf{w}, \mathbf{f} \rangle| + |\langle \mathbf{w}, \mathbf{f} - \tilde{\mathbf{f}} \rangle| + |\langle \mathbf{w} - \tilde{\mathbf{w}}, \tilde{\mathbf{f}} \rangle| \, , \end{aligned} \tag{22}$$

and observing that the RBF cubature formula is trivially exact for every function $z(P)$ in the RBF space associated to $X = \{P_j\}$, i.e.

$$I(z) = \langle \mathbf{w}, \mathbf{z} \rangle \, , \;\; z \in \mathrm{span}\{\phi_j\}_{1 \leq j \leq n} \, , \;\; \mathbf{z} = \{z(P_j)\}_{1 \leq j \leq n} \, , \tag{23}$$

we can write

$$\begin{aligned} |I(f) - \langle \tilde{\mathbf{w}}, \tilde{\mathbf{f}} \rangle| &\leq |I(f) - I(z)| + |\langle \mathbf{w}, \mathbf{z} - \mathbf{f} \rangle| \\ &+ \|\mathbf{w}\|_1 \, \|\mathbf{f} - \tilde{\mathbf{f}}\|_\infty + \|\mathbf{f}\|_2 \, \|A^{-1}(\mathbf{I} - \tilde{\mathbf{I}})\|_2 \, . \end{aligned} \tag{24}$$

Then, we have immediately the estimate

$$\begin{aligned} |I(f) - I(z)| + |\langle \mathbf{w}, \mathbf{z} - \mathbf{f} \rangle| &\leq \mathrm{meas}(\Omega) \, \|z - f\|_\infty + \|\mathbf{w}\|_1 \, \|\mathbf{z} - \mathbf{f}\|_\infty \\ &\leq (\mathrm{meas}(\Omega) + \|\mathbf{w}\|_1) \; \|z - f\|_\infty \, . \end{aligned} \tag{25}$$

Taking the infimum on z in the RBF space, from (24)-(25) we get (21). □

2.1 Optimal recovery and numerical integration.

It is important to mention that the cubature formulae that we have used are *optimal* in the sense of Golomb-Weinberger [15]. To this purpose, it can be proved that the native space $\mathcal{H} = \mathcal{N}_\phi$ relative to the RBF ϕ is indeed a *reproducing kernel Hilbert space* (often abbreviated as RKHS) [1, 27], that in some cases is even norm-equivalent to a Sobolev or a Beppo-Levi space (respectively for the Wendland functions and the Thin-Plate splines).

One can exploit such a property to show that integration by RBF minimizes the norm of the error functional in the dual space $\mathcal{H}^* = \mathcal{N}_\phi^*$. We sketch for simplicity the outline of the proof for RBF with positive definite kernels, but one can easily achieve similar results for conditionally positive radial basis functions and even for more general kernels.

Denoting by δ_P the point evaluation in P and by I the integral functional in (2), it is possible to prove (cf., e.g, [30]) that the minimum of the worst case errors in $\mathcal{H}$ at a given set of centers $\{P_j\}_{j=1,\dots,n}$, i. e. the minimum of

$$\left\| I - \sum_{j=1}^{n} w_j \delta_{P_j} \right\|_{\mathcal{H}^*} = \sup_{f \in \mathcal{H},\, \|f\|=1} \left| I(f) - \sum_{j=1}^{n} w_j\, f(P_j) \right| \tag{26}$$

is attained when the coefficients w_j solve

$$(I, \delta_{P_k})_{\mathcal{H}^*} = \sum_{j=1}^{n} w_j (\delta_{P_j}, \delta_{P_k})_{\mathcal{H}^*},\ k = 1, \dots, n. \tag{27}$$

It is not difficult to show that the Riesz representers of I and δ_P are respectively $v_I := \int_\Omega \phi(|\cdot - Q|) dQ$ and $v_{\delta_P} := \phi(|P - \cdot|)$ from which it easily follows by the definition of the inner product in $\mathcal{H}^*$

$$(I, \delta_P)_{\mathcal{H}^*} = (v_I, v_{\delta_P})_{\mathcal{H}} = \int_\Omega \phi(|P - Q|) dQ\ . \tag{28}$$

Since $\phi(|P - Q|) = (\delta_P, \delta_Q)_{\mathcal{H}^*}$ (see Theorem 1 in [27]), from (27) we get

$$\int_\Omega \phi(|Q - P_k|)\, dQ = \sum_{j=1}^{n} w_j \phi(|P_j - P_k|)\ . \tag{29}$$

As one can immediatly observe, the weights in (29) coincide with those in (10), directly implying that the previous rules are optimal and that they are independent of the function f to integrate.

3 Implementation of RBF cubature.

The error analysis performed in the previous Section is valid for any compact integration domain, which is the closure of an open bounded set satisfying

an interior cone condition. When one turns to the implementation of RBF cubature, a key point is the accurate and efficient evaluation of the integrals of the radial basis functions, and possibly of the polynomial part, in (8).

In the present paper we make a first step towards RBF cubature, considering integration on the unit square $\Omega = [0,1]^2$, where it is possible to exploit conveniently the features of radial basis functions, like radial symmetry, or separation of variables for the Gaussians. This choice is not strongly restrictive, since integration on several bivariate domains and surfaces can be easily reformulated as integration on the unit square by well-known smooth transformations (such as polar coordinates for sectors and generalized sectors, spherical coordinates for the sphere, ...). Moreover, on the square integration of the possible polynomial part in (8) becomes trivial.

3.1 Integrating the Gaussian basis.

Integration of the (scaled) Gaussian basis on the unit square (see (3)-(8)) can be accomplished very effectively, by product splitting and fast computation of the special function

$$\mathrm{erf}(x) = \frac{2}{\sqrt{\pi}} \int_0^x e^{-t^2}\, dt\ . \tag{30}$$

In fact, we can write by separation of variables

$$\int_{[0,1]^2} e^{-|P-P_j|^2/\delta^2}\, dP = \int_0^1 e^{-(x-x_j)^2/\delta^2}\, dx \int_0^1 e^{-(y-y_j)^2/\delta^2}\, dy$$

$$= \frac{\pi\delta^2}{4} \left(\mathrm{erf}\left(\frac{1-x_j}{\delta}\right) - \mathrm{erf}\left(\frac{-x_j}{\delta}\right)\right) \left(\mathrm{erf}\left(\frac{1-y_j}{\delta}\right) - \mathrm{erf}\left(\frac{-y_j}{\delta}\right)\right)\ , \tag{31}$$

and thus we have reduced the problem to computing the special function *erf*, which is efficiently evaluated (up to machine precision) by specific routines available in the most common scientific computing environments [9].

3.2 Integrating other bases by radial symmetry.

In order to integrate the other selected radial bases (TPS, MQ, IMQ, W2, see (3)-(8)) in the Introduction), we can exploit directly the inherent *radial symmetry*. Fixing the interpolation point P_j, we split the unit square with vertices $A = (0,0)$, $B = (1,0)$, $C = (1,1)$, $D = (0,1)$, into four triangles $\mathcal{T}_1 = P_jAB$, $\mathcal{T}_2 = P_jBC$, $\mathcal{T}_3 = P_jCD$, $\mathcal{T}_4 = P_jDA$, and split further for convenience each $\mathcal{T}_k$ into two right triangles $\mathcal{T}_k^{(1)}$, $\mathcal{T}_k^{(2)}$, each one with a vertex in P_j. By the additivity of the integral we get the integral of the radial basis functions as sum of eight integrals

$$\int_{[0,1]^2} \phi_j(P)\, dP = \sum_{k=1}^{4} \sum_{l=1}^{2} \int_{\mathcal{T}_k^{(l)}} \phi_j(P)\, dP\ . \tag{32}$$

At this point, we have only to compute integrals of the form $\int_{\mathcal{T}} \phi_j(P)\, dP$ where $\mathcal{T}$ is a certain right triangle, say $\mathcal{T} = P_j HM$, with the right angle at H (H being the orthogonal projection of P_j on a side of the unit square, and M one of the two vertices of the square on that side); see Fig. 1. Set $r_0 = |P_j - H|$, $r_1 = |P_j - M|$, and denote by θ^* the angle $H\hat{P}_j M$: integrating in polar coordinates,

$$\int_{\mathcal{T}} \phi_j(P)\, dP = \int_0^{\theta^*} \int_0^{r_0/\cos\theta} \phi_j(r\cos\theta, r\sin\theta) r\, dr\, d\theta$$

$$= \int_0^{\theta^*} \int_0^{r_0/\cos\theta} \phi(r/\delta) r\, dr\, d\theta = \delta^2 \int_0^{\theta^*} \Psi\left(\frac{r_0}{\delta\cos\theta}\right) d\theta \;\;,\;\; \theta^* = \arccos\left(r_0/r_1\right) \tag{33}$$

where Ψ is the following primitive

$$\Psi(\rho) = \int_0^{\rho} \phi(r) r\, dr\ , \tag{34}$$

and $r_0/\delta \le r_0/(\delta\cos\theta) \le r_0/(\delta\cos\theta^*) = r_1/\delta \le \sqrt{2}/\delta$. The primitive Ψ is immediately derived analytically

- Duchon's Thin-Plate Splines (TPS): $\Psi(\rho) = \Psi_{\text{TPS}}(\rho) = \frac{\rho^4}{4}\left(\log\rho - \frac{1}{4}\right)$
- Hardy's MultiQuadrics (MQ): $\Psi(\rho) = \Psi_{\text{MQ}}(\rho) = \frac{1}{3}\left((1+\rho^2)^{3/2} - 1\right)$
- Inverse MultiQuadrics (IMQ): $\Psi(\rho) = \Psi_{\text{IMQ}}(\rho) = (1+\rho^2)^{-1/2} - 1$
- Wendland's compactly supported (W2):
  $\Psi(\rho) = \Psi_{\text{W2}}(\rho) = -\frac{1}{7}(1-\rho)_+^5(4\rho^2 + \frac{5}{2}\rho + \frac{1}{2}) + \frac{1}{14}$

In the case of Wendland's W2 radial basis functions, we can derive a formula more suitable for numerical purposes, which takes into account that the support is compact (a disk with radius δ, the scaling parameter). Observe that there are three possible instances, i.e. $\mathcal{T} \cap \text{supp}(\phi_j)$ is either a sector centered at P_j, or the triangle $\mathcal{T}$ itself, or the union of a triangle and a sector having a side in common.

We start considering the last, obtaining the other two as particular cases. Let $\mathcal{T} = P_j HM$ be the right triangle above, and denote by K and J the points where the boundary of the support intersects the sides HM and $P_j M$, respectively. Since $\mathcal{T}$ is the union of the sector $\mathcal{S} = P_j KJ$ (having as radius the scaling parameter δ) with the triangle $\Upsilon = P_j HK$, we have

$$\int_{\mathcal{T}} \phi_j(r/\delta) r\, dr\, d\theta = \int_{\mathcal{S}} \phi_j(r/\delta) r\, dr\, d\theta + \int_{\Upsilon} \phi_j(r/\delta) r\, dr\, d\theta$$

$$= (\theta^* - \theta_\delta) \int_0^{\delta} \phi_j(r/\delta) r\, dr + \int_0^{\theta_\delta} \int_0^{r_0/\cos\theta} \phi_j(r/\delta) r\, dr\, d\theta$$

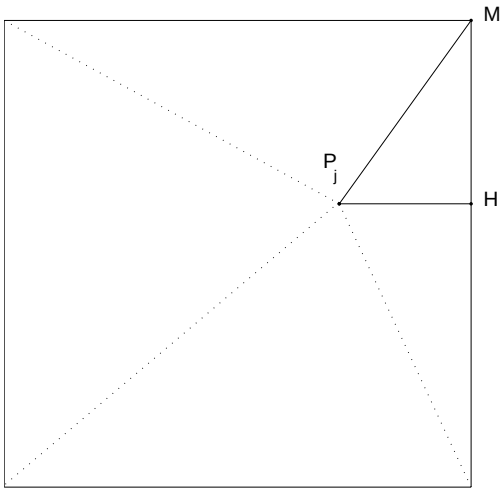

Figure 1: Splitting the square into triangles, for integration of the RBF centered at P_j in polar coordinates.

$$= \delta^2(\theta^* - \theta_\delta) + \delta^2 \int_0^{\theta_\delta} \Psi_{\mathrm{W2}}\left(\frac{r_0}{\delta\cos\theta}\right) d\theta \ , \quad \theta_\delta = \arccos\left(r_0/\delta\right) , \tag{35}$$

where Ψ_{W2} is the restriction to $[r_0/\delta, 1]$, and thus the following polynomial of degree 7

$$\Psi_{\mathrm{W2}}(\rho) = \sum_{k=2}^{7} \alpha_k \, \rho^k = \frac{4}{7}\,\rho^7 - \frac{5}{2}\,\rho^6 + 4\rho^5 - \frac{5}{2}\,\rho^4 + \frac{1}{2}\,\rho^2 \ , \quad \rho \in [0,1] \ . \tag{36}$$

The other two instances are simple consequences of the previous analysis. In fact, it is immediately seen that when $\mathcal{T} \cap \mathrm{supp}(\phi_j) = \mathcal{T}$ then formula (33) directly applies, while if $\mathcal{T} \cap \mathrm{supp}(\phi_j)$ is a sector (necessarily with angle θ^*)

$$\int_{\mathcal{T}} \phi_j(r/\delta) r \, dr \, d\theta = \delta^2 \theta^* \ . \tag{37}$$

With Ψ at hand, the computational problem is now reduced to the evaluation of the last integral in (33) and (35). Due to the ill-conditioning of the collocation matrix (see Section 2), such an integral has to be computed with high accuracy, even up to machine precision for smooth radial functions like MQ and IMQ; see Table 7 below, where we used the `quadl` function of Matlab [14, 21] with different tolerances. Now, since TPS and W2 give the most reliable numerical results (see the next Section), and using an adaptive high-precision integrator like `quadl` hundreds of times creates a bottleneck in the implementation, it is worth deriving *compact formulas* for the corresponding primitives of $\Psi(r_0/(\delta\cos\theta))$.

As for TPS, we have to compute

$$\mathcal{F}_{\text{TPS}}(\theta) = \int \Psi_{\text{TPS}}(a/\cos\theta)\, d\theta = \int \frac{a^4}{4\cos^4\theta} \left(\log\left(\frac{a}{\cos\theta}\right) - \frac{1}{4} \right) d\theta \ , \quad (38)$$

where $a = r_0/\delta$; we recall that, by geometric construction $r_0/\delta \le a/\cos\theta \le a/\cos\theta^* = r_1/\delta \le \sqrt{2}/\delta$. The popular computer algebra system Maple [17] is not able to integrate directly the function of θ above, but after the standard substitution $t = \tan\theta/2$ (cf., e.g., [23]) it succeeds and we finally get

$$\mathcal{F}_{\text{TPS}}(\theta) = \frac{1}{6}\, \frac{a^4}{(1-t^2)^3} \left\{ t(3 - 2t^2 + 3t^4)\, \log\left(\frac{a(1+t^2)}{1-t^2}\right) \right.$$

$$\left. -\frac{t}{12}\,(33 - 38t^2 + 33t^4) - 2\,(1 - 3t^2 + 3t^4 - t^6)\, \arctan\left(\frac{1}{t}\right) \right\} + \frac{\pi}{6}\, a^4 \ ,$$

$$\text{where } \ t = \tan\theta/2 \ , \ \ a = r_0/\delta \ , \quad (39)$$

with $\mathcal{F}_{\text{TPS}}(0) = 0$. Observe that by the representation $\cos\theta = (1-t^2)/(1+t^2)$, (39) can be rewritten as

$$\mathcal{F}_{\text{TPS}}(\theta) = \frac{1}{6}\, \left(\frac{a}{\cos\theta}\right)^3 \frac{a}{(1+t^2)^3} \left\{ t(3 - 2t^2 + 3t^4)\, \log\left(\frac{a}{\cos\theta}\right) \right.$$

$$\left. -\frac{t}{12}\,(33 - 38t^2 + 33t^4) - 2\,(1 - 3t^2 + 3t^4 - t^6)\, \arctan\left(\frac{1}{t}\right) \right\} + \frac{\pi}{6}\, a^4 \ , \quad (40)$$

which shows that by the geometric constraints $\mathcal{F}_{\text{TPS}}(\theta^*) \to 0$ as $\theta^* \to \pi/2$ ($t \to 1$). Recall indeed that the last integral in (33) is exactly $\mathcal{F}_{\text{TPS}}(\theta^*)$, and $\theta^* \to \pi/2$ as $r_0/r_1 \to 0$.

In the case of Wendland's W2 radial basis functions we have by (36) that

$$\mathcal{F}_{\text{W2}}(\theta) = \int \Psi_{\text{W2}}(a/\cos\theta)\, d\theta = \sum_{k=2}^{7} \alpha_k a^k F_k(\theta) \ ,$$

$$\text{where } \ F_k(\theta) = \int \frac{1}{\cos^k\theta}\, d\theta \ , \ \ a = r_0/\delta \ , \quad (41)$$

and the primitives F_k can be computed by the recursive formula (cf. [16])

$$F_k(\theta) = \frac{\sin\theta}{(k-1)\cos^{k-1}\theta} + \frac{k-2}{k-1} F_{k-2}(\theta) \ , \ k > 1 \ , \ \ F_1(\theta) = \log\left|\tan\left(\frac{\theta}{2} + \frac{\pi}{4}\right)\right| . \quad (42)$$

Notice that with the choice $F_0(\theta) = \theta$ we have again $\mathcal{F}_{\text{W2}}(0) = 0$. An explicit expression of $\mathcal{F}_{\text{W2}}(\theta)$ can be obtained by integrating directly $\Psi_{\text{W2}}(a/\cos\theta)$ with Matlab/Symbolic

$$\mathcal{F}_{\text{W2}}(\theta) = \frac{a^2}{84\text{c}^6} \left\{ 8a^5\text{s} + 10a^5\text{sc}^2 + 15a^5\text{sc}^4 + 15a^5\text{c}^6 \log\left((1+\text{s})/\text{c}\right) - 42a^4\text{sc} \right.$$

$$-56a^4\mathrm{sc}^3 - 112a^4\mathrm{sc}^5 + 84a^3\mathrm{sc}^2 + 126a^3\mathrm{sc}^4 + 126a^3\mathrm{c}^6 \log\left((1+\mathrm{s})/\mathrm{c}\right)$$
$$-70a^2\mathrm{sc}^3 - 140a^2\mathrm{sc}^5 + 42\mathrm{sc}^5\Big\} \ , \quad \text{where } \ \mathrm{s} = \sin\theta \ , \ \mathrm{c} = \cos\theta \ . \qquad (43)$$

Now, in view of the geometric constraints $a/\cos\theta^* \leq \sqrt{2}/\delta$, $a/\cos\theta_\delta = 1$, it is easy to show by (43) that $\mathcal{F}_{\mathrm{W2}}(\theta^*) \to 0$ and $\mathcal{F}_{\mathrm{W2}}(\theta_\delta) \to 0$ as $\theta^* \to \pi/2$ ($r_0/r_1 \to 0$) and $\theta_\delta \to \pi/2$ ($r_0 \to 0$), respectively; cf. (33) and (35).

Remark 3.1 The integration procedure for radial basis functions based on radial symmetry is easily adaptable to any *convex polygon*, via domain splitting into triangles; the compact formulas obtained for TPS and W2 remain clearly valid.

4 Numerical results.

In this Section we report a set of numerical results, obtained with Matlab [21], corresponding to the application of five RBF cubature formulas using random points generated with a uniform probability distribution. The RBF are: MultiQuadrics (MQ), Inverse MultiQuadrics (IMQ), Gaussians (G), Wendland's compactly supported (W2), Thin-Plate Splines (TPS).

Table 1. As discussed in Section 2, two important parameters for the analysis of RBF cubature are the spectral norm of the inverse of the (augmented for CPD) collocation matrix, which measures the absolute conditioning of the interpolation and cubature equations, and the 1-norm of the vector of the (computed) weights, i.e. the norm of the RBF cubature functional, which enters the approximation analysis and measures the conditioning of the cubature formula. For each RBF we have considered three values of the scaling parameter δ, corresponding to a variation of three orders of magnitude, due to the fact that the quality of approximation may strongly depend on such a parameter. In particular, decreasing δ has the effect of better conditioning (the separation distance of the scaled points increases), at the price of worsening the error (the fill distance also increases).

We have computed the parameters $\|A^{-1}\|_2$ and $\|\tilde{\mathbf{w}}\|_1$ on sets of $n = 50$ and $n = 100$ uniform random points in the unit square. Since they strongly depend on the particular distribution of the points, we have taken the average values of 50 independent trials (rounded to the *first* significant *digit*). In particular, $\|A^{-1}\|_2$ has been computed by the function `norm` of Matlab [21], which approximates the largest singular value of the matrix.

At first glance we see that the best conditioning is exhibited by the less regular RBF like W2 and TPS, as predicted by the theory concerning $\|A^{-1}\|_2$. It is important to notice that the cubature weights of W2 and TPS are not all positive, but their size is small and the corresponding vector 1-norm is not equal to but still on the order of the measure of the integration

domain. On the other hand, smooth RBF can be (even extremely) ill-conditioned, and can exhibit large values of the 1-norm of the cubature weights. The experience with Matlab and stability analysis suggest that the quantities computed by the built-in function `norm` tend to be underestimates for values bigger than 10^{17}. For this reason, we have used in the next tables the notation "$> E + 17$" for such entries.

Table 1: RBF cubature with sets of $n = 50$ and $n = 100$ random points generated with a uniform probability distribution in $[0, 1]^2$: Spectral norm of the inverses of the collocation matrices and 1-norm of the computed weights vectors (average values on 50 independent trials).

$(n = 50)$	scaling	$MQ(\delta)$	$IMQ(\delta)$	$G(\delta)$	$W2(\delta)$	$TPS(\delta)$
$\|A^{-1}\|_2$	$\delta = 0.1$	4E+03	1E+03	1E+03	2E+01	9E+02
	$\delta = 1$	2E+12	3E+11	5E+15	5E+03	6E+03
	$\delta = 10$	>E+17	>E+17	>E+17	7E+06	6E+05
$\|\tilde{\mathbf{w}}\|_1$	$\delta = 0.1$	2E+00	1E+00	1E+00	2E-01	2E+00
	$\delta = 1$	7E+01	9E+01	3E+02	2E+00	1E+00
	$\delta = 10$	6E+05	6E+04	3E+02	2E+00	1E+00
$(n = 100)$	scaling	$MQ(\delta)$	$IMQ(\delta)$	$G(\delta)$	$W2(\delta)$	$TPS(\delta)$
$\|A^{-1}\|_2$	$\delta = 0.1$	1E+04	5E+03	1E+04	2E+02	9E+02
	$\delta = 1$	2E+16	6E+15	>E+17	5E+04	8E+03
	$\delta = 10$	>E+17	>E+17	>E+17	3E+07	1E+06
$\|\tilde{\mathbf{w}}\|_1$	$\delta = 0.1$	2E+00	2E+00	2E+00	3E-01	1E+00
	$\delta = 1$	8E+02	5E+02	1E+03	2E+00	1E+00
	$\delta = 10$	4E+06	1E+05	6E+02	2E+00	1E+00

Tables 2-3. We report both the RBF interpolation and cubature absolute errors (the former in $\|\cdot\|_\infty$ on a suitable control grid) of two test functions, namely $f(x, y) = \exp(x - y)$ (used also in [20]), and the well-known Franke's test function [13]. As in Table 1, we have taken the average values on 50 independent sets of $n = 50$ and $n = 100$ random points generated with a uniform probability distribution. The integrals of the radial basis functions have been computed as described in the previous section: in particular, for the Gaussians, TPS and W2 we have used the compact formulas derived there, while for MQ and IMQ the one-dimensional integral in (33) has been evaluated to machine precision by the `quadl` function of Matlab [14, 21]. Moreover, for the system of cubature equations (10) we have used the standard direct solver of Matlab (which is based on Gaussian elimination).

A wide set of numerical experiments on the two functions above, as well as on several other test functions (not reported for brevity), revealed that:

- As expected, the quality of the interpolation and of the integration depends strongly on the scaling parameter δ (except for the TPS, cf.

Table 2: Errors of RBF interpolation (E_n^{intp}) and cubature (E_n^{cub}) for the test function $f(x,y) = e^{x-y}$, with $n = 50$ and $n = 100$ random points generated with a uniform probability distribution in $[0,1]^2$ (average values on 50 samples of size n).

	scaling	$MQ(\delta)$	$IMQ(\delta)$	$G(\delta)$	$W2(\delta)$	$TPS(\delta)$
E_{50}^{intp}	$\delta = 0.1$	8E-02	3E-01	8E-01	9E-01	5E-02
	$\delta = 1$	4E-03	8E-03	3E-04	2E-01	6E-02
	$\delta = 10$	1E-03	5E-04	1E-03	3E-02	7E-02
E_{50}^{cub}	$\delta = 0.1$	2E-03	3E-02	3E-01	8E-01	9E-04
	$\delta = 1$	6E-05	1E-04	6E-06	1E-02	2E-03
	$\delta = 10$	7E-01	3E-02	7E-04	4E-04	2E-03
E_{100}^{intp}	$\delta = 0.1$	6E-02	3E-01	5E-01	9E-01	4E-02
	$\delta = 1$	3E-04	8E-04	8E-04	1E-01	2E-02
	$\delta = 10$	2E-03	7E-04	2E-03	2E-02	3E-02
E_{100}^{cub}	$\delta = 0.1$	6E-04	1E-02	8E-02	7E-01	5E-04
	$\delta = 1$	2E-06	5E-06	1E-05	4E-03	2E-04
	$\delta = 10$	4E+00	6E-02	1E-03	1E-04	5E-04

Table 3: As in Table 1, for the Franke's test function.

	scaling	$MQ(\delta)$	$IMQ(\delta)$	$G(\delta)$	$W2(\delta)$	$TPS(\delta)$
E_{50}^{intp}	$\delta = 0.1$	1E-01	2E-01	7E-01	9E-01	1E-01
	$\delta = 1$	1E+00	1E+00	2E+01	9E-02	1E-01
	$\delta = 10$	6E+00	2E+01	1E+01	1E-01	1E-01
E_{50}^{cub}	$\delta = 0.1$	1E-02	2E-02	3E-01	8E-01	1E-02
	$\delta = 1$	4E-02	8E-02	7E-01	7E-03	1E-02
	$\delta = 10$	2E+03	6E+02	7E+00	1E-02	1E-02
E_{100}^{intp}	$\delta = 0.1$	5E-02	1E-01	5E-01	9E-01	6E-02
	$\delta = 1$	1E+01	6E+00	3E+01	7E-02	7E-02
	$\delta = 10$	2E+01	8E+01	2E+01	7E-02	5E-02
E_{100}^{cub}	$\delta = 0.1$	2E-03	8E-03	1E-01	7E-01	3E-03
	$\delta = 1$	2E-01	1E-01	4E-01	2E-03	5E-03
	$\delta = 10$	1E+04	3E+03	2E+01	2E-03	3E-03

[5, p. 1720]); see [24] for a numerical optimization method.

- The cubature error is always smaller than the interpolation error, as is natural.
- In some instances with smooth RBF, good results can be achieved even in presence of high condition numbers (namely with smooth integrands and accurate data).
- TPS and W2 generate the most reliable and robust RBF cubature for-

mulas, which give acceptable results even on moderately large and/or noisy data sets.

Remark 4.1 It is worth trying to explain why, as one observes in Table 1, the cubature weights are still within reasonable limits even when the matrix is extremely ill-conditioned. The main reason is that worst-case bounds like $\|\mathbf{w}\|_2 \leq \|A^{-1}\|_2 \, \|\mathbf{I}\|_2$ (cf. (10)) are very pessimistic, being attained if $\mathbf{I}$ is an eigenvector corresponding to the smallest eigenvalue of A. In fact, numerical experiments with spectra of RBF collocation matrices show that small eigenvalues have eigenvectors with many sign changes. On the other hand, in most cases the vector $\mathbf{I}$ will have only positive components, and thus it maps well into the eigenspaces of the large eigenvalues of A, yielding weights $\mathbf{w} = A^{-1}\mathbf{I}$ with small or moderate size.

5 Conclusions and perspectives.

This paper represents a first step toward a systematic and computationally efficient treatment of RBF numerical cubature on scattered data. Our numerical experiments with some of the most popular RBF on relatively small scattered samples (size up to the hundreds), partially supported by some theoretical considerations and estimates, show that the cubature formulas generated by thin-plate splines and by (suitably scaled) compactly supported radial functions are the most reliable and robust. This is mainly due to the fact that, besides an "acceptable" approximation error, the conditioning of their collocation matrix and of the cubature method have a "reasonable" magnitude (even if the computed cubature weights are not all positive, they are of small size); see Table 1. Moreover, we have eliminated a possible bottleneck of the implementation, by producing compact formulas for the accurate evaluation of their integrals.

A number of computational problems should however be faced. On larger samples (size of the thousands or more), all the computational machinery of RBF should become useful. We try to list some possibilities. On the one hand, the construction of the cubature formulas, which requires solving numerically a linear system with the collocation matrix (the "interpolation equations" for the coefficients or equivalently the "cubature equations" for the weights), has to be accelerated. Within our set of numerical experiments, it has been possible using a standard direct solver, but on large samples conditioning and computational cost can become prohibitive. In such cases one can resort to well-known fast methods for computing the RBF interpolation coefficients like, e.g., preconditioned Krylov subspace methods [8], or domain decomposition strategies [5]. We stress that one could even get trivially a complexity reduction via nonoverlapping domain decomposition, due to the additivity of the integral, but the effect on the quality of cubature should be studied thoroughly.

Another interesting perspective, supported by the good approximation performance shown in our tests, is the use of compactly supported RBF, which leads to sparse collocation matrices and to efficient multilevel solvers [18]. A multilevel approach could also give the possibility of estimating a posteriori the cubature error. Moreover, a multilevel strategy can be useful also to reduce the conditioning on a given sample, without deteriorating too much the approximation. In fact, while the approximation error of RBF interpolation and cubature is related to the smallness of the fill distance (the radius of the inner empty disk), the conditioning suffers from a small separation distance between the nodes. Thinning techniques, as those described in [18], could allow eliminating "redundant" points, i.e. enlarging the separation distance as long as the fill distance remains of the same size. Recall that we ultimately compute a single number (an approximate value of the integral), so a loss of information unacceptable for recovery and/or visualization might be tolerable in the cubature context.

Finally, extension of the cubature method to a larger set of radial basis functions (other compactly supported RBF, polyharmonic splines, ...), and to higher dimension, should be tried. In the latter case, apart from the straightforward case of the Gaussians on multidimensional cubes, evaluating efficiently the integrals of the radial basis functions appears a much more challenging computational problem, compared to the two-dimensional one.

Acknowledgements. The authors wish to thank Dr. Stefano De Marchi, for having introduced them to the fascinating field of radial basis functions. The second author is also grateful to Professor Rick Beatson for a valuable conversation at Padua's antipodes (VIC2004, Wellington), and his encouragement to proceed on the topic of RBF cubature. Special thanks go to the referees, for having improved substantially this paper with their observations. The work was supported by the research project CPDA028291 "Efficient approximation methods for nonlocal discrete transforms" of the University of Padova, by the GNCS-INdAM, and by the MASCOS (ARC Centre of Excellence for Mathematics and Statistics of Complex Systems).

References

[1] N. Aronszajn: Theory of reproducing kernels. Trans. Amer. Math. Soc. 68 (1950), 337-404.

[2] S.N. Atluri, S.P. Shen: The Meshless Local Petrov-Galerkin (MLPG) Method. Tech Science Press, Encino, California, 2002.

[3] K. Ball: Eigenvalues of Euclidean distance matrices. J. Approx. Theory 68 (1992), 74-82.

[4] K. Ball, N. Sivakumar and J.D. Ward: On the sensitivity of radial basis interpolation to minimal distance separation. J. Approx. Theory 68 (1992), 401-426.

[5] R.K. Beatson, W.A. Light and S. Billings: Fast solution of the radial basis function interpolation equations: domain decomposition methods. SIAM J. Sci. Comput. 22 (2000), 1717-1740.

[6] A.Yu. Bezhaev: Cubature formulae on scattered meshes, Soviet J. Numer. Anal. Math. Modelling 6 (1991), 95-106.

[7] M.D. Buhmann: Radial basis functions. Acta Numer. 9 (2000), 1-38.

[8] M.D. Buhmann: Radial Basis Functions: theory and implementation. Cambridge Univ. Press, Cambridge, 2003.

[9] W.J. Cody: Performance evaluation of programs for the error and complementary error functions. ACM Trans. Math. Software 16 (1990), 29-37.

[10] R. Cools and D. Laurie (Eds.): Numerical evaluation of integrals. J. Comput. Appl. Math. 112 (1999), no. 1-2.

[11] G.E. Fasshauer: Meshfree Methods. Handbook of Theoretical and Computational Nanotechnology, M. Rieth and W. Schommers (eds.).

[12] M.S. Floater and A. Iske: Multistep scattered data interpolation using compactly supported radial basis functions. J. Comput. Appl. Math. 73 (1996), 65-78.

[13] R. Franke: Scattered data interpolation: test of some methods. Math. Comp. 38 (1982), 181-200.

[14] W. Gander and W. Gautschi: Adaptive quadrature - revisited. BIT 40 (2000), 84-101.

[15] M. Golomb and H.F. Weinberger: Optimal approximation and error bounds. On numerical approximation. Proceedings of a Symposium, Madison, April 21-23 (1958), 117-190.

[16] I.S. Gradshteyn and I.M. Ryzhik: Tables of integrals, series, and products. Academic Press, Boston, 1994.

[17] A. Heck: Introduction to Maple. 3rd edition, Springer-Verlag, New York, 2003.

[18] A. Iske: Multiresolution Methods in Scattered Data Modelling. Lecture Notes in Computational Science and Engineering, Springer-Verlag, Heidelberg, 2004.

[19] E.J. Kansa, H. Power, G.E. Fasshauer and L. Ling: A Volumetric Integral Radial Basis Function Method for Time-Dependent Partial Differential Equations: I. Formulation. Journal of Engineering Analysis with Boundary Elements 28 (2004), 1191-1206.

[20] D. Levin: Stable integration rules with scattered integration points. Numerical evaluation of integrals. J. Comput. Appl. Math. 112 (1999), 181-187.

[21] Using MATLAB (version 6). The MathWorks, Natick (MA, USA), 2000.

[22] F.J. Narcowich and J.D. Ward: Norms of inverses and condition numbers for matrices associated with scattered data. J. Approx. Theory 64 (1991), 69-94.

[23] N.S. Piskunov: Differential and integral calculus. Mir, Moskow, 1969.

[24] S. Rippa: An algorithm for selecting a good value for the parameter c in radial basis function interpolation. Radial basis functions and their applications, Adv. Comput. Math. 11 (1999), 193–210.

[25] R. Schaback: Error estimates and condition numbers for radial basis function interpolation. Adv. Comput. Math. 3 (1995), 251-264.

[26] R. Schaback: Multivariate interpolation and approximation by translates of a basis function. Approximation theory VIII, Vol. 1 (College Station, TX, 1995), 491-514, Ser. Approx. Decompos. 6, World Sci. Publishing, River Edge, NJ, 1995.

[27] R. Schaback: Native Hilbert Spaces for Radial Basis Functions I. International Series of Numerical Mathematics 132 (1999), Birkhäuser Verlag, 255-282,

[28] R. Schaback: Stability of radial basis function interpolants. Approximation theory, X (St. Louis, MO, 2001), 433-440, Innov. Appl. Math., Vanderbilt Univ. Press, Nashville, TN, 2002.

[29] R. Schaback: Reconstruction of Multivariate Functions from Scattered Data. Monograph (draft, available online at the web site: www.num.math.uni-goettingen.de/schaback/research/group.html).

[30] H. Wendland: Scattered Data Approximation. Cambridge Monographs on Applied and Computational Mathematics, Vol. 17, Cambridge University Press, Cambridge, 2005.

Alvise Sommariva

University of New South Wales
School of Mathematics
Sydney, New South Wales
Australia
e-mail: alvise@maths.unsw.edu.au

Marco Vianello
University of Padua
Department of Pure and Applied Mathematics
Padua
Italy
e-mail: marcov@math.unipd.it